Novel Membrane Processes for the Enantiomeric Resolution of Tryptophan by Selective Permeation Enhancements

Zhengzhong Zhou
Chemical & Pharmaceutical Engineering, Singapore-MIT Alliance, National University of Singapore, Singapore 119260, Singapore

Youchang Xiao
Dept. of Chemical & Biomolecular Engineering, National University of Singapore, Singapore 119260, Singapore

T. Alan Hatton
Dept. of Chemical Engineering, Massachusetts Institute of Technology, Cambridge, MA 02139

Tai-Shung Chung
Dept. of Chemical & Biomolecular Engineering, National University of Singapore, Singapore 119260, Singapore

DOI 10.1002/aic.12336
Published online July 13, 2010 in Wiley Online Library (wileyonlinelibrary.com).

Novel membrane processes for the effective enantioresolution of racemic mixtures have been evaluated. The incorporation of human serum albumin (HSA) in the strip solution of a permeation cell resulted in the partial optical resolution of a racemic tryptophan mixture, as the permeation of L*-tryptophan, which binds to HSA more strongly, was enhanced selectively over that of* D*-tryptophan. A second approach in which a racemic mixture was introduced to the strip solution prior to the experiments showed better performance by selectively decreasing the flux of the more weakly bound* D*-tryptophan. The highest enantioselectivity of ~9.76 was achieved with a third, novel design consisting of two permeation cells in series, which can encompass the advantages of affinity dialysis. An industrial scale unit is proposed based on this concept and a suitably validated mathematical model.* © 2010 American Institute of Chemical Engineers *AIChE J,* 57: 1154–1162, 2011
Keywords: chiral separation, membrane separation, human serum albumin, selective permeation enhancement, enantiomers

Introduction

Optical resolution of enantiomeric drugs has attracted great attention because of the demands for enantiomerically pure drugs from the U.S. food and drug administration and the pharmaceutical industry. Currently, the majority of active pharmaceutical ingredients are chiral in nature and the two enantiomeric forms have different therapeutic effects,[1] which provides the impetus for the development of technologies suitable for chiral separation. Membrane technology, although relatively new in this field compared with the existing techniques such as high-performance liquid chromatography,[2] capillary electrophoresis (CE),[3,4] and preferential crystallization,[5] can be a more cost-effective alternative because it can be scaled up easily as a continuous operation with a higher throughput and lower energy consumption.

Generally, two types of chiral separation have been used in membrane technology. The first type is accomplished with

Correspondence concerning this article should be addressed to T.-S. Chung at chencts@nus.edu.sg.

the aid of a chiral selective membrane, where the membrane is usually functionalized with chiral selectors such as cyclodextrins and their derivatives,[6–9] crown ethers,[10] DNA[11,12], and enzymes[13] that exhibit preferential interaction with one of the enantiomers over the other. The separation of 4-[3-(4-fluorophenyl)-2-hydroxy-1-[1, 2, 4] triazol-1-yl-propyl]-benzonitril performed by Lee et al.[14] is a typical example, where the chiral selectors were physically immobilized within a nanoporous alumina film. Another example is the use of liquid membrane systems where an organic solvent containing chiral selectors, either in bulk[15] or inside the polymeric membrane pores,[16] is used as the liquid membrane. Although a relatively high selectivity can be achieved, the liquid membrane is usually unstable and has a short working life.[17]

The second type of membrane chiral separation is carried out using nonchirally selective membranes coupled with affinity dialysis (AD) concepts, where a specific chiral selector is introduced into the racemic feed solution to form complexes preferentially with one of the enantiomers.[18–20] This mixture is then filtered under pressure by the nonchiral selective membrane with a suitable pore size and surface charge that retains the large complexes. A relatively high enantioseparation can be achieved. For example, chiral selectors such as bovine serum albumin (BSA)[19] and human serum albumin (HSA)[20,21] have shown promising results in tryptophan separation. However, this pressure-driven process is subject to higher operating costs and the performance may deteriorate with membrane fouling. Also, extra post steps are required to separate the chiral selectors and enantiomers in the feed side.

A different approach to membrane-based chiral separations that combines the concepts of liquid membrane technology and AD is used in this study where the chiral selectors are added to the strip solution instead of the racemic feed solution. In a normal diffusion process, the diffusion rate decelerates with time since the concentration gradient across the membrane decreases. With chiral selectors in the strip solution, the enantiomers permeating through the membrane bind to the chiral selectors to different extents depending on their relative association equilibrium constants. As a consequence, not only do we compensate for the deceleration of permeation rate but the deceleration rates themselves also become different, i.e., the permeation deceleration of the more strongly binding enantiomer is lower, resulting in a higher accumulated permeation flux. Enantioselectivity can hence be demonstrated by the selective permeation enhancement (SPE) of the enantiomers. Moreover, this is also different from the normal extraction process by a liquid membrane system where two immiscible solvents are used in the feed and the strip.[22] As all solutions in this work are aqueous, and the chiral selectors are fully constrained to be inside the chamber by the small pore sizes of the membranes, the stability problems associated with ordinary liquid membrane systems can be averted.

The enantioseparation effectiveness of the newly developed SPE approach is examined via three approaches in this study: single permeation cell, two permeation cells in series, and the preaddition of the racemic and chiral selectors to the strip solution. HSA and tryptophan are chosen as the chiral selector and enantiomer pair as the HSA has a high intrinsic

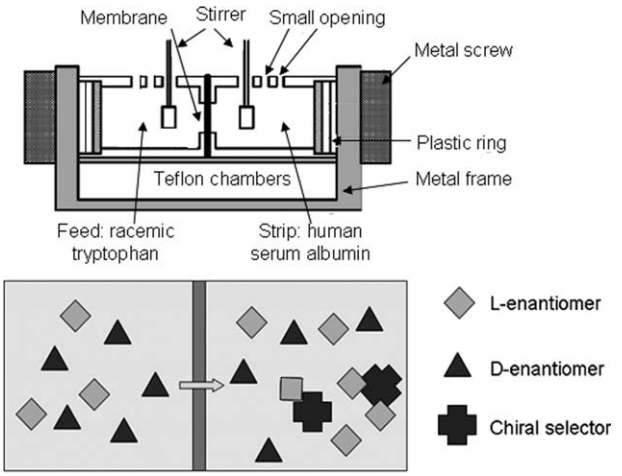

Figure 1. Schematic diagram of SPE with single cell.

selectivity for the resolution of a racemic tryptophan mixture. It has been reported that the L-tryptophan binds to the indol-benzodiazepine site of HSA with an affinity 100 times greater than that of D-tryptophan.[23] Following a demonstration of the feasibility of enantioseparation by the single permeation cell process, the separation performance is further improved by adding a racemic mixture to the strip solution as well; both the selectivity and enantiomeric excess are shown to increase with higher concentrations of racemic mixture preadded to the strip solution. Finally, by connecting two permeation cells in series, we show that the separation performance is greatly enhanced; a new design suitable for industrial application is proposed using hollow fiber membrane modules. Mathematical modeling was exploited to interpret and support the experimental data, through the solution of a set of ordinary differential equations representing the mass balances and reaction equilibria.

Overall, this is an original work that not only demonstrates the model designs of SPE for achieving high enantioselectivity but may also open up new routes and stimulate new ideas for enantiomeric resolution.

Experimental

Materials

The cellulose dialysis membranes Spectro/Pro 7, [molecular cut-off = 1000, membrane thickness = 50 μm) were purchased from Spectrum Medical Industries. HSA and BSA from Sigma–Aldrich, α-cyclodextrin from Cyclolab, DL-tryptophan from Alfa Aesar, and sodium phosphates were all reagent grade and used without further purification.

Chiral separation by SPE in single permeation cell

The chiral separation test was carried out on a dialysis permeation cell setup as shown in Figure 1.[6] The permeation cell was composed of two Teflon chambers between which the dialysis membrane (with area of 9 cm^2) was clamped. The feed was a 35-mL racemic tryptophan solution of 0.1 mM and the strip chamber contained a 35-mL HSA solution at various concentrations (2.5, 5, 10, and 15 g L^{-1}). The pH of each solution was maintained at 8.6 by 20 mM phosphate

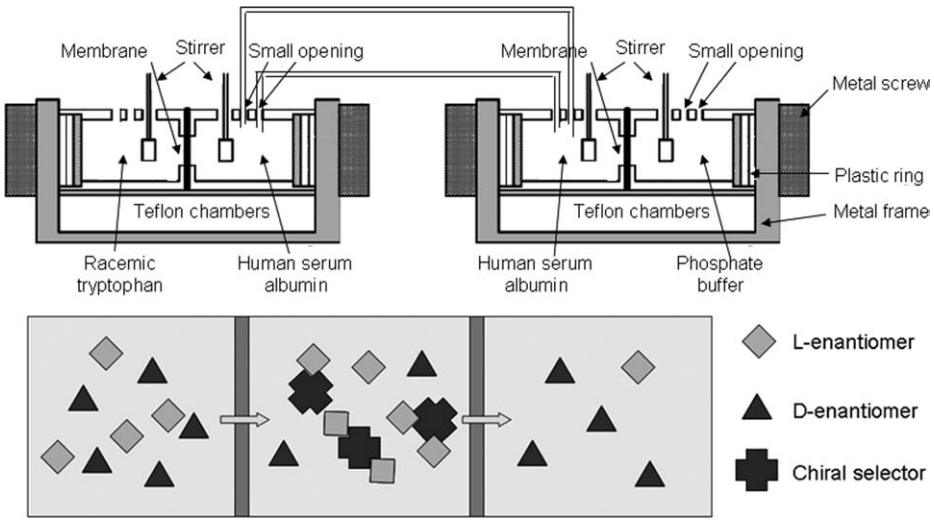

Figure 2. Schematic diagram of SPE-AD unit with two cells in series.

buffer. Two Teflon impellers connected to an overhead stirrer (CAT R18, M. Zipperer GmbH, Staufen, Germany) operating at 200 rpm were used to stir the solutions. Samples (200 μL) were taken from the feed chamber after 22 h and analyzed by CE (P/ACE MDQ CE system, Beckman). The CE buffer was a 50-mM α-cyclodextrin solution with pH maintained at 2.2 by a 20-mM phosphate buffer. The sample injection time was 7.5 s at 0.8 psi and the forward separating voltage was 25 kV. The permeate concentrations were back calculated by subtracting the feed chamber concentration from the original feed solution. The enantiomeric excess and selectivity was calculated with the following equations:

$$\text{ee}\% = \frac{C_D - C_L}{C_D + C_L} \times 100\% \tag{1}$$

$$\alpha = \frac{Q_L}{Q_D} = \frac{(F_L - C_L) \bullet V/t}{(F_D - C_D) \bullet V/t} = \frac{(F_L - C_L)}{(F_D - C_D)} \tag{2}$$

where ee% represents the enantiomeric excess of the retentate and α is the apparent selectivity of the SPE system, defined as the ratio of the flux of L-tryptophan permeating through the membrane to that of D-tryptophan, C_L, C_D, F_L, and F_D are the L-tryptophan and D-tryptophan concentrations in the retentate and in the original feed solution, respectively, V is the solution volume in the strip chamber, t is the permeation time, while Q_L and Q_D are the fluxes of enantiomers.

Chiral separation by SPE with preaddition of feed

The experimental procedures were similar to those described in the previous section except that a racemic enantiomer mixture was added, with concentration varying up to that of the feed, together with the HSA, into the strip solution. The mixture in the strip solution was prepared 4 h before permeation experiments to ensure equilibrium. The difference in the concentration gradients of the two enantiomers across the membrane could then be increased from the beginning of the experiment, and in such a way, products with higher enantiomeric excess were harvested from the feed chamber.

Chiral separation by SPE in two permeation cells in series

The setup consisted of two permeation cells in series as shown in Figure 2. The contents of cell 1 were similar to those used in the single cell test, while the two chambers of cell 2 contained HSA solution and phosphate buffer, respectively. The protein chambers of the two cells were connected with a circulating pump, such that the solution concentrations of the two chambers could be assumed to be the same. Samples (200 μL) were withdrawn periodically from the strip side, analyzed by CE, and thereafter inject back into the strip side to maintain an almost constant volume.

Control experiments of AD

In the AD control experiments, 10 g L^{-1} HSA were added directly to the feed solution and formed complexes with enantiomers which were retained by the membrane. The permeation experiment was conducted 4 h after solution preparation to ensure equilibrium. Samples were then taken from the strip solution periodically and tested by CE.

Mathematical modeling of permeation tests

Matlab 7.4.0 was used for the calculation of theoretical permeation results. The set of standard mass balance and equilibrium equations listed below was solved with the aid of the built in function "ode45."

$$V_1 \frac{dC_{L1}}{dt} = -\frac{AD}{d}(C_{L1} - C_{L2}) \tag{3}$$

$$V_1 \frac{dC_{D1}}{dt} = -\frac{AD}{d}(C_{D1} - C_{D2}) \tag{4}$$

$$V_2 \frac{dC_{L2}}{dt} = \frac{AD}{d}(C_{L1} - 2C_{L2} + C_{L3}) - V_2\left(k_L C_{L2} P - k'_L P_{CL}\right) \tag{5}$$

$$V_2 \frac{dC_{D2}}{dt} = \frac{AD}{d}(C_{D1} - 2C_{D2} + C_{D3}) - V_2\left(k_D C_{D2} P - k'_D P_{CD}\right) \tag{6}$$

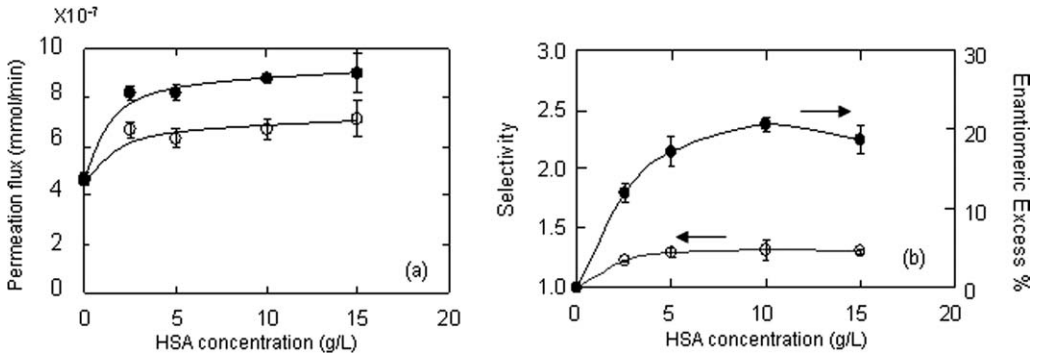

Figure 3. (a) Permeation fluxes of tryptophan against HSA concentration in strip; (b) enantioselectivity and enantiomeric excess (ee%) of the retentate against HSA concentrations in strip with single cell SPE.

$$V_1 \frac{dC_{L3}}{dt} = \frac{AD}{d}(C_{L2} - C_{L3}) \quad (7)$$

$$V_1 \frac{dC_{D3}}{dt} = \frac{AD}{d}(C_{D2} - C_{D3}) \quad (8)$$

$$\frac{dP}{dt} = -\left(k_L C_{L2} P - k_L' P_{CL}\right) - \left(k_D C_{D2} P - k_D' P_{CD}\right) \quad (9)$$

$$\frac{dP_{CL}}{dt} = \left(k_L C_{L2} P - k_L' P_{CL}\right) \quad (10)$$

$$\frac{dP_{CD}}{dt} = \left(k_D C_{D2} P - k_D' P_{CD}\right) \quad (11)$$

where V, A, d, t, and C represent the solution volume, membrane effective area, membrane thickness, permeation time, and concentration, respectively, D denotes the apparent diffusion constant derived from experiments, and k_L, k_L', k_D, and $k_D'$are association and dissociation constants between HSA and DL-tryptophan obtained from literature sources.[24] The subscripts 1, 2, and 3 denote the feed chamber, HSA chambers, and strip chamber, respectively, while subscripts L, D, CL, CD refer to the L-tryptophan, D-tryptophan, HSA, HSA-L-tryptophan complex, and HSA-D-tryptophan, respectively.

Results and Discussion

The concepts for the enhanced optical resolution of racemic mixtures proposed in this article were tested experimentally using the membrane permeation cells described above. In this section, we discuss the overall performance of the three configurations and propose ways in which they might be used industrially.

SPE performance by single cell permeation

The transmembrane fluxes of tryptophan were enhanced with addition of HSA into the strip chamber as shown in Figure 3a. This was expected as HSA formed complexes with tryptophans such that the free tryptophan concentrations in the strip chamber were suppressed to a low level and the concentration gradients were maintained. A general increasing trend of flux with HSA concentration was also observed due to the more complexes formed with more concentrated HSA.

As the concentration gradient was the only driving force in this experiment, the initial permeation rates of both enantiomers were similar. However, on formation of the HSA–tryptophan complexes on the permeate side according to the two equilibrium reactions

$$\text{HSA} + \text{L} - \text{tryp} \leftrightarrow \text{HSA} - \text{L} - \text{tryp} \quad \text{(A)}$$

$$\text{HSA} + \text{D} - \text{tryp} \leftrightarrow \text{HSA} - \text{D} - \text{tryp} \quad \text{(B)}$$

the free enantiomer concentrations in the strip solution were reduced. As HSA is more selective to L-tryptophan, naturally more L-tryptophan was bound to form complexes and the free L-tryptophan concentration was reduced to a greater extent than was the D-tryptophan concentration. A higher concentration gradient of L-tryptophan across the membrane was therefore maintained, which resulted in a higher overall permeation flux of L-tryptophan, i.e., selectivity of L-tryptophan against D-tryptophan. This effect is clearly evident in the data shown in Figure 3b, calculated with Eqs. 1 and 2; furthermore, it is also shown in Figure 3b that the separation performance increased with an increase in HSA concentration in the strip solution, consistent with expectations, because a high HSA concentration shifts the equilibrium concentrations in reactions A and B further to the right, such that the permeation fluxes of both enantiomers are enhanced. However, due to the stronger binding between HSA and L-tryptophan, a preferential concentration decrease of the free L-tryptophan prevailed, thus enhancing enantioselectivity.

It was also noted that the ee% and selectivity decreased when HSA concentration was too high as indicated by the results obtained with 15 g L^{-1} of HSA. One possible reason could be that the binding of D-tryptophan is also greatly enhanced in too great an excess of HSA as reflected in the equilibria given in reactions A and B. As a result, the increment of D-tryptophan flux across the membrane was steadily maintained while the flux of L-tryptophan had almost reached its maximum as the free L-tryptophan concentration was close to zero. Hence, we observed that both ee% and selectivity obtained using this approach were maximized at an intermediate value of HSA concentration, i.e., further improvements in separation performance cannot be achieved by simply increasing the HSA concentration. New approaches were designed and are presented in the following sections.

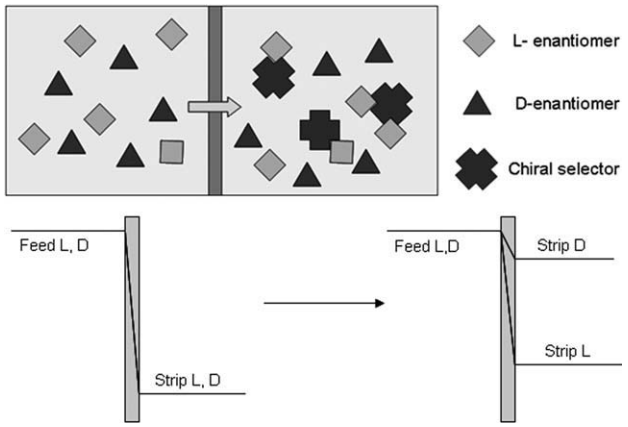

Figure 4. Schematic diagram of enantiomer separation with prefeed addition (upper); schematic representation of change in concentration gradient by prefeed addition (bottom).

SPE performance by single cell permeation with preaddition of feed

Although the enantiomers could be partitioned successfully in the experiments outlined above, one shortcoming was the low selectivity near the beginning of the experiment when both enantiomer concentrations in the permeate side were close to zero and their driving forces were similar. The overall selectivity was therefore compromised. A higher enantioselectivity would be possible if a difference in driving forces could be induced from the beginning of the experiments. Therefore, in the subsequent experiments, while the HSA concentration in the permeate (or strip) side was maintained at 10 g L^{-1}, certain concentrations of racemic enantiomer mixtures were also added to the permeate side prior to the permeation experiment. Under these conditions, the initial driving force (i.e., concentration gradient) for the L-tryptophan was higher than that for the D-tryptophan as the HSA/L-tryptophan complexes formed preferentially on the permeate side so that the actual concentration of free D-tryptophan was higher than the free L-tryptophan concentration in the strip solution, as depicted in Figure 4.

The permeation results from such experiments are presented in Figures 5a, b. It is evident that the results support our hypothesis very well as both ee% in the final feed solution and selectivity were improved, with a commensurately higher concentration of racemic tryptophan in the strip solution. With a higher free D-tryptophan than L-tryptophan concentration in the permeate side, the reduction in permeation flux of D-tryptophan was much stronger than that in the flux of L-tryptophan. This agreed well with Figure 5a, which showed a greater increment in D-tryptophan yield from the feed chamber, as reflected in its steeper increase with increasing concentration of preadded tryptophan. As a result, both the selectivity of L/D-tryptophan and the ee% of the retentate increased with an increase in the concentration of the racemic tryptophan mixture added to the permeate side.

The effect of HSA concentration on enantioseparation performance was also studied by fixing the preadded racemic tryptophan concentration at 0.1 mM and varying the HSA concentration on the permeate side. The results in Figures 5c, d show a generally decreasing trend in tryptophan yield

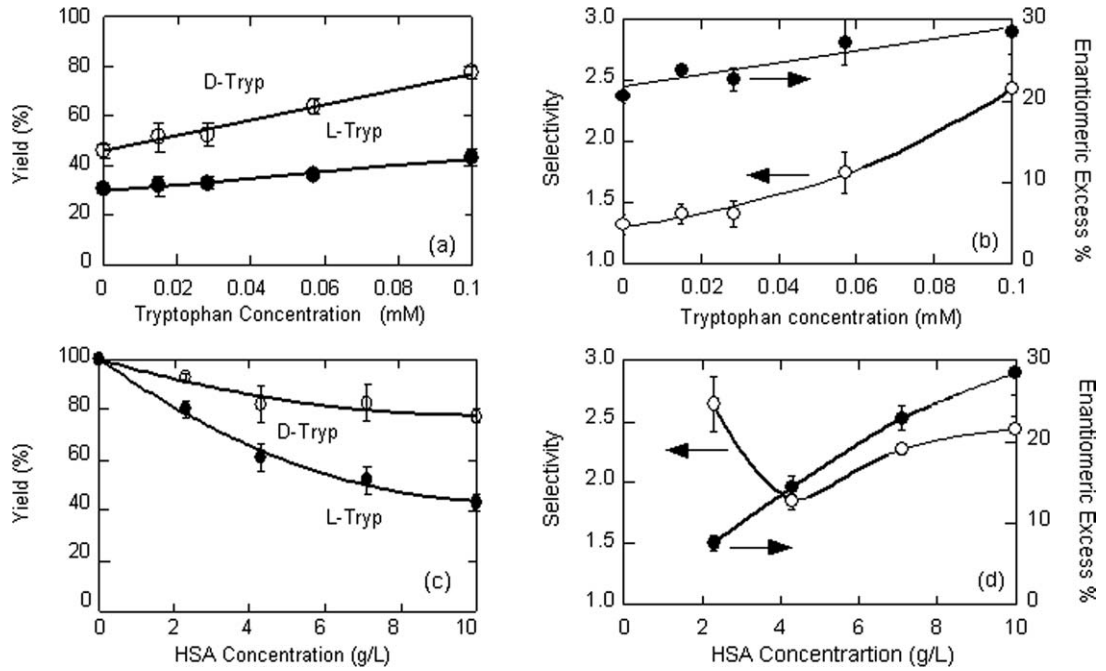

Figure 5. Trends of yield, enantioselectivity, and enantiomeric excess (ee%) in single cell SPE process with preaddition of racemic feed in strip.

(a) Yield of tryptophan from feed chamber in 22 h vs. preadded tryptophan concentration in strip; (b) Selectivity and ee% vs. preadded tryptophan concentration in strip; (c) Yield of tryptophan from feed in 22 h vs. HSA concentration in strip; (d) Selectivity and ee% vs. HSA concentration in strip.

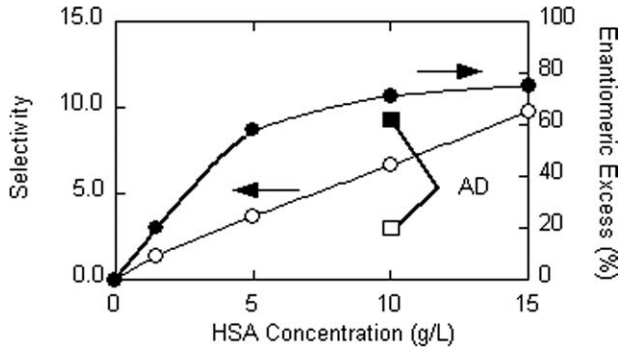

Figure 6. Enantioselectivity and enantiomeric excess with various HSA concentrations in central chambers. AD, affinity dialysis.

from the feed chamber but increasing trends in ee% in the final feed solutions and selectivity with HSA concentration, attributed primarily to the preferential permeation enhancement of L-tryptophan induced by the complex formation with HSA, as explained above. However, the selectivity at the lowest HSA concentration was higher than that at other HSA concentrations within the range of experiments. This interesting observation may be attributed to competitive binding between L-tryptophan and D-tryptophan with HSA in the strip side solution when the HSA concentration (0.035 mM) is lower than the preadded racemic enantiomer concentration (0.1 mM). Because of the selective binding of HSA with L-tryptophan, the permeation of D-tryptophan did not increase as much as that of L-tryptophan, resulting in a high selectivity in the L/D-tryptophan separation.

Overall, the effect of HSA addition to the strip solution was to increase the driving force for the permeation flux of enantiomers, with a significantly greater enhancement in the case of L-tryptophan. On the other hand, the effect of preaddition of feed in the strip was to decrease the permeation flux of enantiomers but more so for D-tryptophan, which resulted cooperatively in higher enantioselectivities.

SPE performance by two permeation cells in series

Although fair enantioseparations were attained in the processes described above, they were considerably inferior to the optimized affinity ultrafiltration (AUF) systems reported by researchers such as Romero and Zydney[20] (selectivity ~7). In a typical AUF process, the complexes formed by incorporating a large enantioselective binding agent into a racemic feed solution can be retained by a membrane with a suitable pore size. Consequently, a higher transmembrane flux of the less strongly bound enantiomer is achieved, with good ee% in the filtrate and, after the removal of the binding agent, in the retentate. For comparison, an AD process that mimicked an AUF system without a transmembrane pressure was carried out together with an SPE process using 10 g L^{-1} of HSA and 0.1 mM racemic tryptophan mixtures. The selectivity and ee% in the AD approach can reach up to 3.01 and 62%, respectively, while the maximum selectivity and ee% are 1.3 and 20%, respectively, in the SPE approach.

To overcome this limitation, we have introduced a novel synergizing strategy by connecting an SPE and an AD unit in series as depicted in Figure 2, which in turn provides an outstanding enantioseparation performance in comparison to that of each respective unit alone. The new approach can integrate the advantages of both SPE and AD systems successfully. In the SPE unit on the left side, the enantiomers first diffuse from the feed chamber into the HSA chamber, with a higher permeation flux of L-tryptophan as discussed

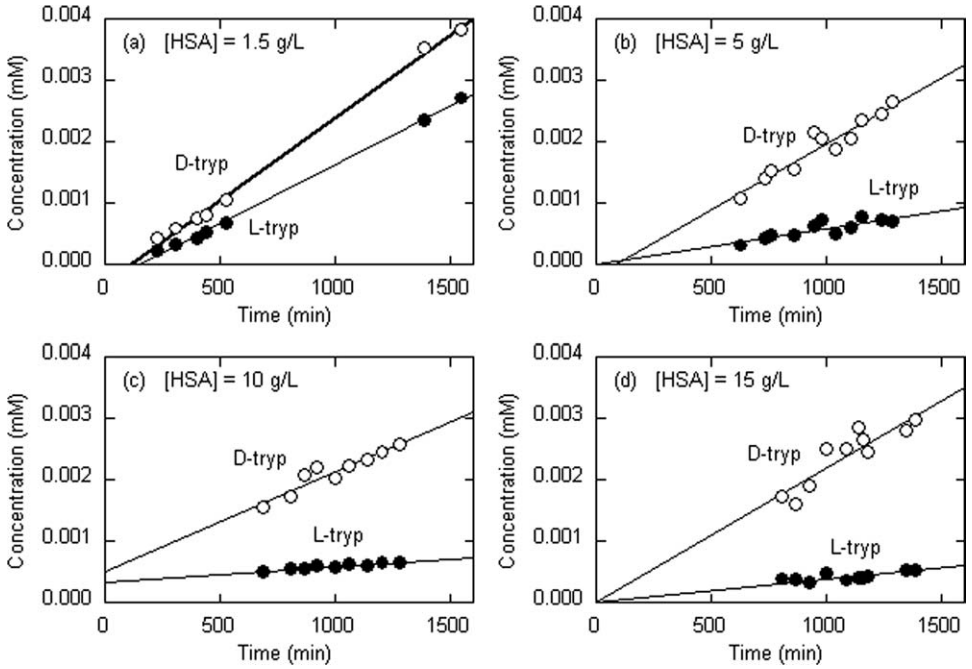

Figure 7. Graphs of tryptophan concentrations over time in the third chamber with the HAS concentrations in the central chamber being (a) 1.5 g L^{-1}; (b) 5 g L^{-1}; (c) 10 g L^{-1}; (d) 15 g L^{-1}.

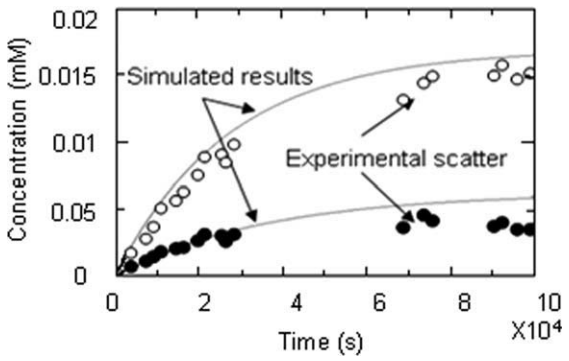

Figure 8. Simulated and experimental results of affinity dialysis with 10 g L^{-1} HSA.

in the previous sections. Thus, while the total concentration of L-tryptophan in the HSA chamber was higher than that of D-tryptophan, the free L-tryptophan concentration was lower as most of the L-tryptophan was bound to HSA. This resulted in a higher concentration gradient of free D-tryptophan than of free L-tryptophan across the membrane in the AD unit on the right side. Hence, the output strip solution of the AD unit showed an enantiomeric excess of D-tryptophan, which was higher than that of the single SPE and AD processes operating individually, as shown in Figure 6.

As the free enantiomer concentrations in the HSA chamber were suppressed by the complex formation with HSA, the flux into the strip chamber of the AD unit was relatively small; thus, the permeate product concentration in the third chamber could be assumed to be linear with time, as shown by the straight lines in Figure 7. The permeability coefficients were therefore calculated from the slopes of these lines using the equation

$$P = \frac{GVd}{A(C_F - C_S)} \tag{12}$$

where G, V, d, and A are the gradient, strip chamber volume, membrane thickness, and membrane area, respectively. C_F and C_S are the corresponding enantiomer concentrations in the feed and strip chambers. The selectivity is the ratio of the enantiomer permeability coefficients, and as other parameter values were the same for both enantiomers, it was calculated from the ratio of gradients only.

$$\alpha = \frac{P_D}{P_L} = \frac{G_D}{G_L} \tag{13}$$

It should be noted that the ee% of the strip solution was calculated instead of that of the retentate in the feed chamber as done in the previous section, as the direct product from the setup was the strip solution, which had a higher ee%. Equation 10 was used by replacing the retentate concentration with the strip concentration.

It is expected that the separation performance of the SPE-AD system would outperform the normal AD system while keeping other conditions equal, as it was observed that higher selectivity and ee% of the product were obtained given the same HSA concentration of 10 g L^{-1}. One possible explanation was the instantaneous high HSA to enantiomer ratio in the middle protein chamber. In our control AD experiments, the ratio was around 3:2 (0.15 mM:0.1 mM) and slowly increased as the enantiomers permeated through the membrane; however, this value was much larger in the SPE-AD system. In the HSA chambers, the initial HSA concentration was also 0.15 mM while the initial tryptophan concentration was zero and slowly increased with time, resulting in a much higher overall HSA to tryptophan ratio. As a consequence, the free L-tryptophan concentration in the HSA chamber was maintained always at a very low level due to the formation of a complex with HSA. Thus, a high selectivity was achievable due to the low permeation of L-tryptophan.

A similar reasoning can be applied to explain the increasing trend in selectivity and ee% with higher HSA concentrations in the middle protein chambers. The increased HSA to enantiomer ratio with an increase in HSA concentration in the middle chamber decreased the free L-tryptophan concentration in the middle chamber to a greater extent, while the free D-tryptophan concentration was less affected due to its weaker complexation with the HSA. Hence, the permeation of L-tryptophan into the strip chamber was greatly reduced, resulting in a higher enantioselectivity of D-tryptophan over L-tryptophan.

Overall, the complete process can also be viewed as a liquid membrane system where the HSA chamber was the liquid membrane with chiral selectors immobilized in the bulk solution. However, this process exhibits much higher stability relative to common liquid membranes. In this newly proposed process, contamination of the product by the liquid membrane solvent was eliminated as DI water was used as the sole solvent within the experiments. The cellulose membrane pore size was about 1 nm, much smaller than the size of HSA, and thus contamination by chiral selector leakage was highly unlikely as well.

Modeling of permeation processes

As the concentration gradient was the only driving force for transport across the membranes, and the cellulose membrane was hydrophilic, membrane fouling was negligible in these experiments. The diffusion constant was calculated simply from the data of one control experiment. The initial conditions were 0.1 mM racemic tryptophan in the feed chamber and phosphate buffer without HSA in the strip solution; samples from the feed and strip chambers were taken periodically and analyzed by CE. The set of Eqs. 3 and 4, together with

$$V_2 \frac{dC_{L2}}{dt} = \frac{AD}{d}(C_{L1} - C_{L2}) \tag{14}$$

$$V_2 \frac{dC_{D2}}{dt} = \frac{AD}{d}(C_{D1} - C_{D2}) \tag{15}$$

was used to find D, with an initial D value calculated from the gradient of permeate concentration against time, and a built in function "fminsearch," the diffusion constant was estimated to be 3.57×10^{-4} cm^2 s^{-1}.

The association and dissociation constants between HSA and L,D-tryptophan were obtained from the work of Yang and Hage.[24] The validity of these constants, together with the calculated diffusion constant, was supported by the close

agreement of the a priori predictions with experimental results shown in Figure 8 for the control AD experiments.

A representative simulation of the SPE in series, with a protein concentration of 10 g L^{-1}, is depicted in Figure 9, again showing good agreement between the experimental and modeling results. This result not only validates the model but also, to a certain extent, the accuracy of the experimental data and the applicability of the SPE system. With this model, it would be possible theoretically to optimize the experimental conditions to achieve the desired separation performance for any pair of chiral selectors and enantiomers as long as their diffusion, association, and dissociation constants were available.

Design for large scale applications

As the driving force for the two cells in series design was the concentration gradient only, and the effective membrane area in our experiments was small, the overall permeation flux was relatively low; with the same experimental conditions and 10 g L^{-1} HSA, the permeability coefficients of L-tryptophan and D-tryptophan of an AD process were 4.97×10^{-8} cm s^{-1} and 1.5×10^{-7} cm s^{-1}, respectively, whereas that of an SPE-AD process were only 0.16×10^{-8} cm s^{-1} and 1.05×10^{-8} cm s^{-1}. Thus, a simple, direct scale-up would not be suitable for real industrial application despite its high enantioselectivity. Inspired by the module designs in other applications,[25–28] we propose an improved design making use of hollow fiber membranes instead; the schematic diagram, which is a modification of that for an internally staged permeator,[25] is shown in Figure 10. The racemic feed and the strip solution flow in the lumen side of each of the two separate bundles of hollow fiber membranes, while the stream containing the chiral selectors flows on the shell side. This design has at least two advantages in comparison to the current experimental setup that greatly increase the permeation flux of the enantiomers. First, the total effective membrane area of hollow fibers is much larger than that of the flat membranes. Second, the hollow fibers in which the feed and strip solutions flow can be closely packed such that the diffusion distance of the enantiomers is shortened. Hence, this new design can lead to a much higher permeation flux while maintaining the enantioselectivity. Moreover, the flow rate and concentration of each stream can be optimized with the aid of mathematical modeling by adopting mass balance equations for processes involving hollow fiber membranes.

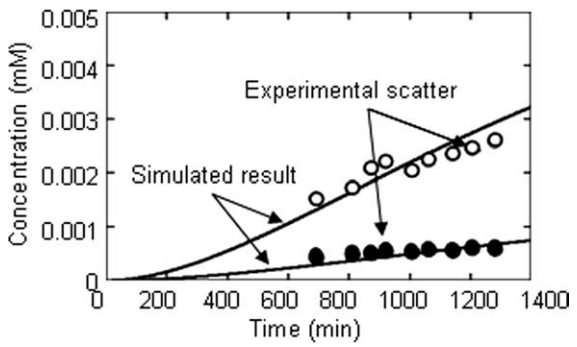

Figure 9. Simulated and experimental results of SPE with two cells in series at HSA concentration of 10 g L^{-1}.

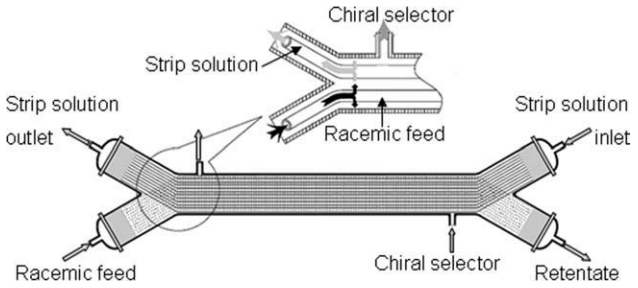

Figure 10. Schematic diagram of enantioseparation for industrial application (modified from Li's work [25]).

Conclusions

In our systematic search for efficient enantioseparation processes, we have studied the performance of a novel operation, SPE, using three different approaches: single cell permeation, preaddition of feed, and two cells in series permeation. The feasibility of SPE was first demonstrated successfully in the single cell permeation system where trends in selectivity and ee% were elucidated, but limitations on the overall performance were also discovered. These limitations were overcome by the preaddition of some of the feed solution to the strip solution; better performance was achieved and an increase in the selectivity and ee% with increasing preadded feed solution was observed. The enantioseparation performance was further enhanced by exploiting the SPE concept using two cells in series to give selectivities of up to 9.76 and corresponding enantiomeric excesses of up to 75%. These performance metrics can be improved further by using a more concentrated HSA solution. This impressive performance was also predicted by the simulation results. The overall rates of the enantiomeric separation were rather slow in the experimental systems studied because of the small membrane areas relative to the volumes being treated, this limitation can be readily overcome using hollow fiber membrane systems, with two bundles of fibers (for the feed and the stripping solutions) being separated by the chiral selector solution in the shell of the module; this new design should provide for a greatly increased throughput.

Acknowledgments

The authors thank the Singapore-MIT Alliance and the National University of Singapore (Grant No. R-279-000-249-646) for funding this project. They also thank Dr. Li Yi for his invaluable suggestions.

Literature Cited

1. Maier NM, Franco P, Linder W. Separation of enantiomers: needs, challenges, perspectives. *J Chromatogr A*. 2001;906:3–33.
2. Ravelet C, Peyrin E. Recent developments in the HPLC enantiomeric separation using chiral selectors identified by a combinatorial strategy. *J Sep Sci*. 2006;29:1322–1331.
3. Wistuba D, Schurig V. Enantiomer separation of chiral pharmaceuticals by capillary electrochromatography. *J Chromatogr A*. 2000;875:255–276.

4. Wang Z, Ouyang J, Baeyens WRG. Recent developments of enantioseparation techniques for adrenergic drugs using liquid chromatography and capillary eletrophoresis: a review. *J Chromatogr B*. 2008;862:1–14.
5. Li JZ, Grant DJW. Relationship between physical properties and crystal structures of chiral drugs. *J Pharm Sci*. 1997;86:1073–1078.
6. Xiao Y, Lim HM, Chung TS, Raj R. Acetylation of β-cyclodextrin surface-functionalized cellulose dialysis membranes with enhanced chiral separation. *Langmuir*. 2007;23:12990–12996.
7. Xiao Y, Chung TS. Functionalization of cellulose dialysis membranes for chiral separation using beta-cyclodextrin immobilization. *J Membr Sci*. 2007;290:78–85.
8. Zhou Z, Xiao Y, Chung TS, Hatton TA. Effects of spacer arm length and benzoation on enantioseparation performance of β-cyclodextrin functionalized cellulose membranes. *J Membr Sci*. 2009;339: 21–27.
9. Yudiato A, Dewi E, Kokugan T. Separation of isomers by ultrafiltration using modified cyclodextrins. *Sep Purif Tech*. 2000;19:103–112.
10. Kakuchi T, Takaoka T, Yokota K. Polymeric chiral crown ether 6 optical resolution of alpha-amino-acid by polymers incorporating 1,3-4,6-di-O-benzylidene-D-mannitol residues. *Polym J*. 1990;22: 199–205.
11. Higuchi A, Hayashi A, Kanda N, Sanui K, Kitamura H. Chiral separation of amino acids in ultrafiltration through DNA-immobilized cellulose membranes. *J Mol Struct*. 2005;739:145–152.
12. Higuchi A, Higuchi Y, Furuta K, Yoon BO, Hara M, Maniwa S, Saitoh M, Sanui K. Chiral separation of phenylalanine by ultrafiltration through immobilized DNA membranes. *J Membr Sci*. 2003;221: 207–218.
13. Lakshmi BB, Martin CR. Enantioseparation using apoenzymes immobilized in a porous polymeric membrane. *Nature*. 1997;388:758–760.
14. Lee SB, Mitchell DT, Trofin L, Navanen TK, Soderlund H, Martin CR. Antibody-based Bio-nanotube membranes for enantiomeric drug separation. *Science*. 2002;296:2198–2200.
15. Morishima I, Lizuka T. Enantiomer differentiation in transport through bulk liquid membranes. *J Am Chem Soc*. 1974;96:7367–7369.
16. Bryjak M, Koziowski J, Wieczorek P, Kafarski P. Enantioselective transport of amino acid through supported chiral liquid membranes. *J Membr Sci*. 1993;85:221–228.
17. Armstrong DW, Jin HL. Enrichment of enantiomers and other isomers with aqueous liquid membrane containing cyclodextrin carriers. *Anal Chem*. 1987;59:2237–2241.
18. Garnier F, Randon J, Rocca JL. Enantiomeric separation by ultrafiltration: complexation mechanism of tryptophan analogs to bovine serum albumin. *Sep Purif Tech*. 1999;16:243–250.
19. Higuchi A, Hara M, Horiuchi T, Nakagawa T. Optical resolution of amino acids by ultrafiltration membranes containing serum albumin. *J Membr Sci*. 1994;93:157–164.
20. Romero J, Zydney AL. Staging of affinity ultrafiltration processes for chiral separation. *J Membr Sci*. 2002;209:107–119.
21. Wang H, Li Y, Chung TS. A fine match between the stereoselective ligands and membrane pore size for enhanced chiral separation. *AIChE J*. 2009;55:2284–2291.
22. Tang K, Chen Y, Huang K, Liu J. Enantioselective resolution of chiral aromatic acids by biphasic recognition chiral extraction. *Tetrahedron: Asymmetry*. 2007;18:2399–2408.
23. Mcmenamy RH, Oncley JL. The specific binding of L-tryptophan to serum albumin. *J Biol Chem*. 1958;233:1436–1447.
24. Yang J, Hage DS. Role of binding capacity versus binding strength in the separation of chiral compounds on protein-based high-performance liquid chromatography columns interaction of D- and L-tryptophan with human serum albumin. *J Chromatogr A*. 1996;725: 273–285.
25. Li D, Wang R, Chung TS. Fabrication of lab-scale hollow fiber membrane modules with high packing density. *Sep Purif Tech*. 2004;40:15–30.
26. Liu B, Lipscomb GG, Jensvold J. A comparison of optimal internally staged permeator and external two-staged module designs for O_2 enrichment from air. *Sep Sci Technol*. 2001;36:2385–2409.
27. Sidhoum M, Sengupta A, Sirkar KK. Asymmetric cellulose acetate hollow fibers: studies in gas permeation. *AIChE J*. 1988;34:417–425.
28. Li K, Acharya DR, Hughes R. Simulation of gas separation in an internally staged permeator. *Chem Eng Res Des*. 1991;69:35–42.

Manuscript received Oct. 6, 2009, revision received Mar. 22, 2010, and final revision received Jun. 11, 2010.